

# Constraints on Dark Energy Models Including Gamma Ray Bursts

Hong Li<sup>1</sup>, Meng Su<sup>1</sup>, Zuhui Fan<sup>1</sup>, Zigao Dai<sup>2</sup> and Xinmin Zhang<sup>3</sup>

<sup>1</sup> *Department of Astronomy, School of Physics, Peking University, Beijing, 100871, P. R. China*

<sup>2</sup> *Department of Astronomy, Nanjing University, Nanjing 210093, P. R. China and*

<sup>3</sup> *Institute of High Energy Physics, Chinese Academy of Science, P.O. Box 918-4, Beijing 100049, P. R. China*

In this paper we analyze the constraints on the property of dark energy from cosmological observations. Together with SNe Ia Gold sample, WMAP, SDSS and 2dFGRS data, we include 69 long Gamma-Ray Bursts (GRBs) data in our study and perform global fitting using Markov Chain Monte Carlo (MCMC) technique. Dark energy perturbations are explicitly considered. We pay particular attention to the time evolution of the equation of state of dark energy parameterized as  $w_{DE} = w_0 + w_a(1 - a)$  with  $a$  the scale factor of the universe, emphasizing the complementarity of high redshift GRBs to other cosmological probes. It is found that the constraints on dark energy become stringent by taking into account high redshift GRBs, especially for  $w_a$ , which delineates the evolution of dark energy.

## I. INTRODUCTION

Cosmological observations, including Type Ia supernovae (SNe Ia)[1, 2, 3, 4], Cosmic Microwave Background radiation (CMB)[5, 6], Large-Scale Structures (LSS)[7] and so on, have provided strong evidence for a spatially flat universe being in a stage of accelerating expansion. In the context of Friedmann-Robertson-Walker cosmology, this acceleration is attributed to a new form of energy with negative pressure, dubbed dark energy (DE), whose nature remains a big puzzle. The simplest candidate for DE is the cosmological constant. However, it suffers from the notorious fine tuning and coincidence problems [8, 9]. Many dynamical models on DE, such as quintessence [10, 11, 12, 13], phantom [14], k-essence [15, 16] and quintom, have been proposed to avoid above difficulties. Among them, the quintom model allows the equation of state (EOS) crossing -1 during evolution [17]. Extensive studies on this model has been carried on both theoretically and phenomenologically [17, 18, 19, 20, 21, 22, 23, 24, 25, 26, 27, 28, 29, 30, 31, 32, 33, 34, 35, 36, 37, 38].

Different DE models predict different global evolutions as well as different structure formations of the universe. Therefore cosmological observations can provide important constraints on the nature of DE. However, degeneracies of cosmological parameters exist in almost all cosmological observations, i.e., they are sensitive not to single parameters but to some specific combinations of them. It is therefore highly necessary to combine different probes to break parameter degeneracies so as to achieve tight cosmological constraints. Furthermore, different observations are affected by different systematic errors, and it is thus helpful to reduce potential biases by combining different probes. To perform joint analyzes, global fitting is the most secure study, because it avoids using strong, and sometimes even inappropriate priors obtained from other observations.

Observations on SNe Ia have played important roles in DE studies[2, 3, 4]. However, due to the difficulties of detecting high-redshift SNe Ia, such a geometrical measurement is limited. The future SNAP/JDEM is planed to probe up to redshift around  $z \sim 2$ . On the other hand, the 3-year WMAP data (WMAP3), which is so far the most precise measurement of the CMB, reveals the information about our universe at redshift around  $z \sim 1100$ . In between, there have not been many probes accessible to us. In this regard, GRBs are the most promising tracers of the evolution of the universe at redshift around a few to even a few tens because they are the most powerful events in the universe. The currently operating Swift satellite is able to detect about 100 long duration GRB events within one year, and we expect that it will open up a potentially new window for GRB cosmographic studies. At present, the measured redshifts of GRBs have extended to  $z = 6.29$ [39]. Even though the physical origin of the long GRB is not very clear, many extensive discussions about the relations between the spectral and temporal parameters show the potential for using long GRBs as cosmic candles for cosmography.

Recently, headway has been made in considering how to make GRBs standard candles. In the literature there are many studies about the intrinsic correlations between temporal or spectral properties of GRBs and their isotropic energies and luminosities, for example, the spectral lag – the luminosity correlation ( $\tau - L_{iso}$ )[40], the luminosity – variability correlation ( $V - L_{iso}$ )[41], the spectral peak energy – isotropic energy correlation ( $E_{peak} - E_{iso}$ )[42], the peak spectral energy – isotropic luminosity correlation ( $E_{peak} - L_{iso}$ )[43] and the isotropic luminosity – peak energy – high signal time scale correlation ( $L_{iso} - E_{peak} - T_{0.45}$ )[44] and so on. These correlations help GRBs nearly to be "known candles" [45]. Shaefer obtained the first GRB Hubble diagram of 9 GRBs with known redshift by using the spectral lag and the variability indicators, and from the GRB hubble diagram he constrained  $\Omega_m < 0.35$  within  $1\sigma$  confidence level[46]. After that, many investigations have been triggered on using GRBs as cosmological probes [47, 48, 49, 50, 51, 52, 53, 54, 55]. Very recently, Shaefer[56] has constructed a GRB Hubble Diagram with 69 GRBs

over a redshift range of 0.17 to  $> 6$ , with 39 GRBs having redshifts  $z > 1.5$ . It is the largest GRB sample so far. The aim of this paper is to present a more general analysis on the EOS of DE by including GRB data in addition to CMB, LSS and SNe Ia in global fitting. We mainly consider the dynamical dark energy parameterization for there is no compelling reason to neglect the evolution of dark energy factitiously. We employ MCMC techniques for the analysis. The MCMC method is the global fitting on the cosmological parameters and we use the original CMB and LSS data rather than use the CMB shift parameter, the linear growth factor or the Baryon Acoustic Oscillation (BAO) measured from the Large scale structure survey. The global fitting is the most secure way for processing data because it is a joint analysis and it can avoid using some strong or even inappropriate priors from others. The effects of dark energy perturbations are carefully taken into account with great attention paid to the perturbations when the equation of state gets across -1. Our paper is structured as follows: in Section II we describe the method and the data; in Section III we present our results on the determination of cosmological parameters from global fitting; finally we present our conclusions in Section V.

## II. METHOD AND DATA

In this section we describe the method used in the fitting process. For the DE parametrization, we adopt  $\Lambda$ CDM model, constant  $w$  and pay particular attention to the commonly used EOS of the form[57]:

$$w_{DE}(a) = w_0 + w_a(1 - a) \quad (1)$$

where  $a = 1/(1 + z)$  is the scale factor and  $w_a$  characterizes the “running” of the EOS. The evolution of DE density is then

$$\rho_X(a)/\rho_X(a_0 = 1) = a^{-3(1+w_0+w_a)} \exp[3w_a(a - 1)] . \quad (2)$$

For DE models whose EOS is not equal to  $-1$ , the perturbation inevitably exists. The perturbation of DE has no effect on the geometric constraints of SN Ia, however, for the CMB and LSS data, the perturbation of DE should be considered, because the late time ISW effects differ significantly when DE perturbation are considered, and the ISW effects take an important part on large angular scales of CMB and the matter power spectrum of LSS[22]. For quintessence-like or phantom-like models where  $w$  does not cross  $-1$ , there are not fundamental difficulties in dealing with perturbations. In parameter fitting, however, biases may be introduced if we limit our considerations only to quintessence or only to phantom models. Thus it is more natural and consistent to allow  $w$  crossing  $-1$  in the fitting analysis. Furthermore, there are observational indications that  $w$  might evolve from  $w > -1$  in the past to  $w < -1$  at present, which have stimulated many theoretical studies. For  $w$  crossing  $-1$ , one is encountered with the divergence problem for perturbations at  $w = -1$ . For handling the parametrization of the EOS getting across -1, firstly we introduce a small positive constant  $\epsilon$  to divide the full range of the allowed value of the EOS  $w$  into three parts: 1)  $w > -1 + \epsilon$ ; 2)  $-1 + \epsilon \geq w \geq -1 - \epsilon$ ; and 3)  $w < -1 - \epsilon$ . Working in the conformal Newtonian gauge, the perturbations of DE can be described by

$$\dot{\delta} = -(1 + w)(\theta - 3\dot{\Phi}) - 3\mathcal{H}(c_s^2 - w)\delta , \quad (3)$$

$$\dot{\theta} = -\mathcal{H}(1 - 3w)\theta - \frac{\dot{w}}{1 + w}\theta + k^2\left(\frac{c_s^2\delta}{1 + w} + \Psi\right) . \quad (4)$$

Neglecting the entropy perturbation, for the regions 1) and 3), the EOS does not across  $-1$  and the perturbation is well defined by solving Eqs.(3,4). For the case 2), the perturbation of energy density  $\delta$  and divergence of velocity,  $\theta$ , and the derivatives of  $\delta$  and  $\theta$  are finite and continuous for the realistic quintom DE models. However for the perturbations of the parameterizations, there is clearly a divergence. In our study for such a regime, we match the perturbations in region 2) to the regions 1) and 3) at the boundary and set

$$\dot{\delta} = 0 , \quad \dot{\theta} = 0 . \quad (5)$$

In our numerical calculations we limit the range to be  $|\Delta w = \epsilon| < 10^{-5}$  and find our method to be a very good approximation to the multi-field quintom. More detailed treatments can be found in Ref.[22].

The publicly available Markov Chain Monte Carlo (MCMC) package CosmoMC[58] is employed in our global fitting, and modifications have been made to include DE perturbations, and to suit the DE models which we study. We assume purely adiabatic initial conditions and work in the flat universe with  $\Omega_{total} = 1$ . Our most general parameter space is:

$$\mathbf{P} \equiv (\omega_b, \omega_c, \Theta_s, \tau, w_0, w_a, n_s, \ln(10^{10} A_s)) \quad (6)$$

Table I. Mean  $1\sigma$  constraints on the EOS of DE and  $\Omega_m$ . The left columns are obtained with “WMAP3+SDSS+2dFGRS+SN<sub>gold</sub>+GRBs” combinations and the right columns are correspondingly from without GRBs.

	WMAP3+LSS+SN <sub>gold</sub> +GRBs			WMAP3+LSS+SN <sub>gold</sub>		
	$\Lambda$ CDM	constant w	dynamical w(a)	$\Lambda$ CDM	constant w	dynamical w(a)
$w_0$	-1	$-0.853^{+0.077}_{-0.076}$	$-1.005^{+0.153}_{-0.151}$	-1	$-0.863^{+0.077}_{-0.076}$	$-1.001^{+0.166}_{-0.162}$
$w_a$	0	0	$0.533^{+0.454}_{-0.474}$	0	0	$0.443^{+0.527}_{-0.550}$
$\Omega_m$	$0.290^{+0.020}_{-0.020}$	$0.285^{+0.021}_{-0.020}$	$0.292^{+0.021}_{-0.021}$	$0.286^{+0.020}_{-0.021}$	$0.283^{+0.020}_{-0.021}$	$0.288^{+0.021}_{-0.021}$

where  $\omega_b \equiv \Omega_b h^2$  and  $\omega_c \equiv \Omega_c h^2$  are the baryon and cold dark matter densities relative to the critical density,  $\Theta_s$  is the ratio (multiplied by 100) of the sound horizon at decoupling to the angular diameter distance to the last scattering surface,  $\tau$  is the optical depth due to re-ionization,  $w_0$  and  $w_a$  is the parameters of the EOS of DE,  $A_s$  and  $n_s$  characterize the power spectrum of primordial scalar perturbations. For the  $\Lambda$ CDM,  $w_0 = -1, w_a = 0$ ,

We vary the above parameters and fit to the observational data with the MCMC method. For the pivot of the primordial spectrum we set  $k_{s0} = 0.05 \text{Mpc}^{-1}$ . The following weak priors are taken:  $\tau < 0.8$ ,  $0.5 < n_s < 1.5$ ,  $-3 < w_0 < 3$ , and  $-5 < w_a < 5$ . We impose a tophat prior on the cosmic age as  $10 \text{ Gyr} < t_0 < 20 \text{ Gyr}$ . Furthermore, we make use of the HST measurement of the Hubble parameter  $H_0 = 100 h \text{ km s}^{-1} \text{Mpc}^{-1}$  by multiplying the likelihood by a Gaussian likelihood function centered around  $h = 0.72$  with a standard deviation  $\sigma = 0.08$ [59]. We also adopt a Gaussian prior on the baryonic density  $\Omega_b h^2 = 0.022 \pm 0.002$  ( $1 \sigma$ ) from Big Bang Nucleosynthesis[60].

In our calculations, we take the total likelihood to be the products of the separate likelihoods ( $\mathcal{L}_i$ ) of CMB, LSS, SNIa and GRB. Defining  $\chi^2_{L,i} \equiv -2 \log \mathcal{L}_i$ , we then have

$$\chi^2_{L,total} = \chi^2_{L,CMB} + \chi^2_{L,LSS} + \chi^2_{L,SNIa} + \chi^2_{L,GRBs} . \quad (7)$$

If the likelihood function is Gaussian,  $\chi^2_L$  coincides with the usual definition of  $\chi^2$  up to an additive constant corresponding to the logarithm of the normalization factor of  $\mathcal{L}$ . For CMB, we include the three-year WMAP (WMAP3) data and compute the likelihood with the routine supplied by the WMAP team [6]. For LSS, we use the 3D power spectrum of galaxies from SDSS [61] and from 2dFGRS[62]. To minimize the nonlinear effects, we restrict ourselves only to the first 14 bins when using the SDSS results[63], the range of  $k$  is  $0.01578 < k/h < 0.10037$ . For SNe Ia, we mainly present the results with the recently released “gold” set of 182 supernovae published by Riess *et al.* in Ref.[4]. For the GRB data, we have considered the published sample by Schaefer[56], which includes 69 GRB events. Upon using these distance modulus, we notice the circulation problem associated with GRBs for cosmological probing. Due to the lack of the local calibration, usually the correlations depend on the cosmological parameters that we attempt to constrain. However, there are results that show the relation does not change dramatically in a wide range of cosmological parameters[64]. In this paper we do not adopt the correction for the circulation problem, and we take the distance modulus published by Schaefer. In the calculation of the likelihood from SNe Ia and GRBs data, we marginalize over the nuisance parameter[65, 66].

For each regular calculation, we run 8 independent chains comprising of 150,000–300,000 chain elements, and spend thousands of CPU hours on a supercomputer. The average acceptance rate is about 40%. We test the convergence of the chains by Gelman and Rubin criteria[67] and find that  $R - 1$  is on the order of 0.01, which is much more conservative than the recommended value  $R - 1 < 0.1$ .

### III. RESULTS AND DISCUSSIONS

In this section, we present our global fitting results. We summarize the  $1\sigma$  constraints on the corresponding parameters in Table I. We focus on the EOS of DE and  $\Omega_m$ . In order to show explicitly the effects of GRBs, we compare the results between the two cases with or without GRBs. From the Table, we can see that the best fit values and the errors change when the GRBs data are included, especially on the parameters of the EOS of DE. For  $\Lambda$ CDM or constant  $w$  DE models, the best fit values and the errors change little when considering the GRBs data, however, for the dynamical DE models, the effects from GRBs can be obviously seen. The best fit value of  $(w_0, w_a)$  is  $(-1.001, 0.443)$  for the combined SN Ia + WMAP3 + SDSS + 2dFGRS. When we adopt the GRBs data, the best fit value of  $(w_0, w_a)$  changed to  $(-1.005, 0.533)$ , and the error bars shrink considerably, especially on  $w_a$  which delineate the evolution of DE. One can find that the  $2\sigma$  error bar of  $w_a$  changed from  $0.443^{+0.747}_{-1.502}$  to  $0.553^{+0.663}_{-1.318}$ , which is tightened about 15%. This can be seen in Fig 1 graphically.

In Figure 1, we delineate the two dimensional posterior constraint on  $w_0 - w_a$ . The solid lines and the dashed lines stand for  $1\sigma$  and  $2\sigma$  constraints respectively. We divide the parameter space into four regions representing different

dark energy models by two lines:  $w_0 = -1$  and  $w_0 + w_a = -1$ . For models located in the upper left region labeled as Quintom A, the equation of state of dark energy crosses  $-1$  from upside down, i.e.,  $w$  is greater than  $-1$  in the past and becomes less than  $-1$  at present. The evolution of  $w$  for models of Quintom B has an opposite direction. From the plot, it is noted that Quintom A models are mildly favored by current observational data. The  $\Lambda$ CDM model continues to be a consistent one at  $2\sigma$  level with and without GRBs included.

The parameter  $w_a$  represents the evolution of DE. It is known that the CMB data alone cannot constrain well the dynamics of DE. LSS data are valuable in DE studies mostly because they provide a tight limit on  $\Omega_m$ , which in turn helps to constrain the properties of DE due to the degeneracy between  $\Omega_m$  and the EOS of DE in cosmological observables. Currently the measurements of the luminosity-distance from SNe Ia at various redshifts give rise to the most direct constraints on the dynamics of DE. In a flat universe with the EOS of DE given by Eq. (1), the luminosity distance can be written as

$$d_L = c(1+z) \int_0^z \frac{dz'}{H_0[\Omega_m(1+z')^3 + (1-\Omega_m)(1+z')^{3(1+w_0+w_a)} \exp[-3w_a \frac{z'}{1+z'}]]^{\frac{1}{2}}}. \quad (8)$$

From this equation, one can see that there are degeneracies between the background parameters  $w_0$ ,  $w_a$ ,  $\Omega_m$  and  $H_0$ . In figure 2 we present the degeneracy by exploring the information of luminosity distance at different redshifts in the  $w_0 - w_a$  parameter plane. Different colored bands describe the parameter space of  $w_0, w_a$  where the variation of  $d_L$  is in between  $\pm 1\%$  for  $z = 0.1$  (black),  $0.5$  (red),  $1$  (green),  $2$  (blue),  $3$  (cyan),  $10$  (magenta) and  $1100$  (yellow). One can find that the degeneracy between  $w_0$  and  $w_a$  varies with the redshift, which in turn implicit that combining the information of  $d_L$  at different redshifts can help break such a degeneracy. Therefore, in order to constrain the cosmological parameters well, one needs distance determinations for a wide range of redshifts. For current SNe Ia data, the redshift range is limited with the highest observed redshift  $\sim 1.7$ . On the other hand, for the GRB sample used in our analysis, the redshift extends to as high as  $\sim 6.3$  with 39 data points having  $z > 1.5$ , thus, the complementarity of GRBs to SNe Ia is highly expected. This plot is the ideal case for showing the degeneracy between the parameters  $w_0$  and  $w_a$  for different redshift, because we fix the other parameters except  $w_0$  and  $w_a$ . In fact, if we vary the other parameters like  $\Omega_m$  or  $H_0$ , the changing of the degeneracy with redshift will also exist but will not be so obvious as figure 2, the different colored bands will be much broader than the ones in figure 2 respectively. Figure 1 is more general results which is obtained from the global fitting where we have all the parameters in equation (6) varying.

To demonstrate the degeneracies between different parameters, we show in Figure 3 the two-dimensional correlation contours of  $w_0$ ,  $w_a$  and  $\Omega_m$  from our global fitting. It is seen that, with the GRBs data, the constraints on the parameters are tightened to a certain degree, especially for  $w_0$  and  $w_a$ . Our results show that high-redshift cosmological probes can play roles in the study of the dynamics of dark energy, and thus it is of importance to explore high-redshift cosmological probes.

GRBs can bridge up the gap between the relatively nearby SN Ia and the much earlier CMB. Comparing with SN Ia, GRBs have their own advantages. They are very powerful and thus can be detected out to very high redshifts. Furthermore, the gamma-ray photons suffer from no dust extinction when they propagate to us. Therefore they deserve detailed studies. Although the cosmological applications of GRBs are currently limited by the relatively small number of available data and the quality of the data, it is considerably important to investigate their potentials and related problems. With the accumulation of observational data and the advances of theoretical understandings of GRB physics, the goal of using GRBs as cosmological candles could be better achieved.

#### IV. SUMMARY

In this paper, we have made the first global fitting with the combined GRB, WMAP3, SDSS, 2dFGRS and SN Ia data. We concentrate on dynamical DE models, and explore the complementarity of GRBs to other cosmological probes. DE perturbations are treated carefully. From the global fitting results given by MCMC, we find that high-redshift GRBs may have effects in constraining the EOS of DE, especially for the dynamical DE models. Including GRBs data can shrink the contours and modify the best fit values of DE parameters. The  $\Lambda$ CDM model is consistent with the current data within  $2\sigma$  confidence level, with Quintom A-like models mildly favored.

GRBs are the most powerful astrophysical events in the universe, which hold great potential to reveal the high redshift universe. Even though, the GRB data are not as good as SN Ia currently, our results indicate the possible potentials of GRBs in dark energy studies.

It is worth mentioning that our global fitting method is different from using the CMB shift parameter, the linear growth factor or the BAO parameter measured from the LSS. Although these parameters carry important information of dark energy, their specific values are usually extracted from observational data under certain conditions. Overlooking these conditions leads to inappropriate use of the values of these parameters, which in turn could result biased

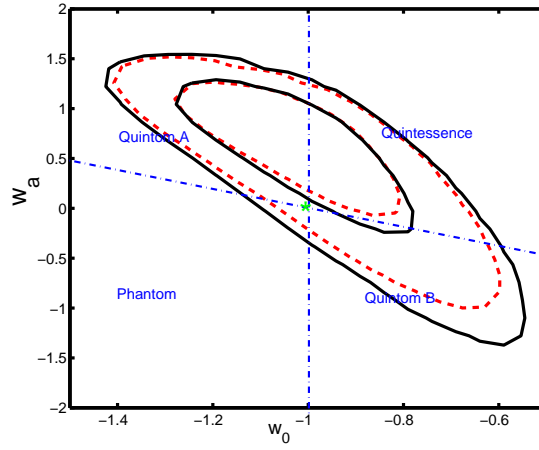


FIG. 1:  $2\sigma$  constraints in the  $w_0$  and  $w_a$  plane, the dotted red line is given by using WMAP3+182 "Gold" SNIa+LSS+GRBs with our 8-parameter parametrization discussed in the text. Solid black curves come from without GRBs. For both cases we considered perturbed dark energy.

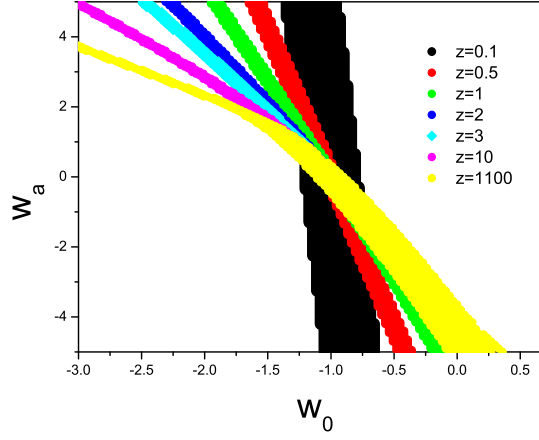


FIG. 2: The different color region simple  $\pm 1\%$  variation around lines of constant  $d_L$  at redshift 0.1 (black), 0.5 (red), 1 (green), 2 (blue), 3 (cyan), 10 (magenta), 1100 (yellow), taking  $\Lambda$  CDM model as fiducial model. This plot delineate the degeneracy between the parameters  $w_0$  and  $w_a$  at different redshift  $z$ .

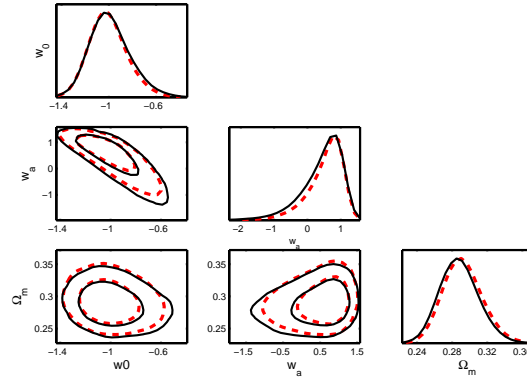


FIG. 3: 1-d posterior constraints and 2-d joint 68% and 95% confidence regions for the parameters  $w_0$ ,  $w_a$  and  $\Omega_m$  obtained via MCMC methods. The dotted red line is given by using WMAP3+182 "Gold" SNIa+LSS+GRBs while the solid black curves come from without GRBs. For both cases we considered perturbed dark energy.

constraints on cosmological parameters. Our MCMC analysis are performed on observational data directly and therefore avoid such problems. We also take into account dark energy perturbations, whose effects are not included in the shift parameter and the BAO parameter.

The analysis presented in this paper mainly aims at emphasizing the importance of high-redshift cosmological probes, which are not limited to GRBs. Our results demonstrate their contributions to dark energy studies clearly, especially on the dynamics of the dark energy component.

### Acknowledgments

Our MCMC chains were finished in the Sunway system of the Shanghai Supercomputer Center(SSC). Hong Li thanks the Center de Physique des Particules de Marseille for the kind hospitality during part of the preparation of this work and acknowledges the funding support from the China postdoctoral science foundation. This work is supported in part by National Science Foundation of China under Grant Nos. 90303004, 19925523, 10243006, 10373001, 10233010, 10221001 and 10533010, and by Ministry of Science and Technology of China under Grant No. NKBRSF G19990754 and TG1999075401, by the Key Grant Project of Chinese Ministry of Education (No. 305001). We thank Junqing Xia, Gong Bo Zhao, Bo Feng, Jingsong Deng, Charling Tao and F. Virgili for helpful discussions.

- 
- [1] S. Perlmutter et al., *Astrophys. J.* **483** (1997) 565.
  - [2] A. G. Riess et al., *Astrophys. J.* **116** (1998) 1009.
  - [3] A. G. Riess et al., *Astrophys. J.* **607** (2004) 665.
  - [4] A. G. Riess *et al.*, astro-ph/0611572.
  - [5] D. N. Spergel et al., *Astrophys. J. Suppl.* **148** (2003) 175.
  - [6] D. N. Spergel, et al., astro-ph/0603449.
  - [7] U. Seljak et al., *Phys. Rev. D* **71** (2005) 103515.
  - [8] S. Weinberg, *Rev. Mod. Phys.* **61** (1989) 1.
  - [9] I. Zlatev, L.-M. Wang, and P. J. Steinhardt, *Phys. Rev. Lett.* **82** (1999) 896.
  - [10] R. D. Peccei, J. Sola and C. Wetterich, *Phys. Lett. B* **195** (1987) 183.
  - [11] C. Wetterich, *Nucl. Phys. B* **302** (1988) 668.
  - [12] B. Ratra and P. J. E. Peebles, *Phys. Rev. D* **37** (1988) 3406.
  - [13] P. J. E. Peebles and B. Ratra, *Astrophys. J.* **L17** (1988) 325.
  - [14] R. R. Caldwell, *Phys. Lett. B* **545** (2002) 23.
  - [15] T. Chiba, T. Okabe and M. Yamaguchi, *Phys. Rev. D* **62** (2000) 023511.
  - [16] C. Armendariz-Picon, V. F. Mukhanov and P. J. Steinhardt, *Phys. Rev. Lett.* **85** (2000) 4438.
  - [17] B. Feng, X. L. Wang and X. M. Zhang, *Phys. Lett. B* **607** (2005) 35.
  - [18] B. Feng, M. Li, Y. S. Piao and X. Zhang, *Phys. Lett. B* **634** (2006) 101.
  - [19] J. Q. Xia, B. Feng, and X. Zhang, *Mod. Phys. Lett. A* **20** (2005) 2409.
  - [20] J. Q. Xia, G. B. Zhao, B. Feng, H. Li and X. Zhang, *Phys. Rev. D* **73** (2006) 063521.
  - [21] J. Q. Xia, G. B. Zhao, B. Feng and X. Zhang, astro-ph/0603393;  
J. Q. Xia, G. B. Zhao, H. Li, B. Feng and X. Zhang, astro-ph/0605366.
  - [22] G. B. Zhao, J. Q. Xia, M. Li, B. Feng and X. Zhang, *Phys. Rev. D* **72** (2005) 123515.
  - [23] G. B. Zhao, J. Q. Xia, B. Feng and X. Zhang, astro-ph/0603621.
  - [24] M. z. Li, B. Feng and X. m. Zhang, *JCAP* **0512** (2005) 002.
  - [25] X. F. Zhang, H. Li, Y. S. Piao and X. M. Zhang, *Mod. Phys. Lett. A* **21** (2006) 231.
  - [26] X. F. Zhang and T. Qiu, astro-ph/0603824.
  - [27] Z. K. Guo, Y. S. Piao, X. M. Zhang and Y. Z. Zhang, *Phys. Lett. B* **608** (2005) 177.
  - [28] H. Wei and R.-G. Cai, hep-th/0501160.
  - [29] Y. F. Cai, H. Li, Y. S. Piao, and X. Zhang, gr-qc/0609039.
  - [30] A. A. Andrianov, F. Cannata and A. Y. Kamenshchik, gr-qc/0505087.
  - [31] X. Zhang and F. Q. Wu, *Phys. Rev. D* **72** (2005) 043524;  
Z. Chang, F. Q. Wu, and X. Zhang, *Phys. Lett. B* **14** (2006) 633;  
X. Zhang, *Phys. Rev. D* **74**, (2006) 103505.
  - [32] B. McInnes, *Nucl. Phys. B* **718** (2005) 55.
  - [33] I. Y. Aref'eva, A. S. Koshelev, and S. Yu. Vernov, astro-ph/0507067.
  - [34] J. Grande, J. Sola and H. Stefancic, gr-qc/0604057.
  - [35] L. P. Chimento and R. Lazkoz, astro-ph/0604090.
  - [36] F. Cannata and A. Y. Kamenshchik, gr-qc/0603129.
  - [37] R. Lazkoz and G. Leon, astro-ph/0602590.
  - [38] H. Stefancic, astro-ph/0511316.

- [39] Kawai et al., CGN (2005) 3937.
- [40] Norris, Marani and Bonnel, APJ **534** (2000) 248.
- [41] Lamb, Graziani and Smith, APJ **L11** (1993) 413.
- [42] L. Amati et al., A & A **81** (2002) 390.
- [43] Yonetoku et al., APJ **395** (2004) 609.
- [44] Firmani et al., astro-ph/0605073.
- [45] G. Ghirlanda, G. Ghisellini, and C. Firmani, New J.Phys. **8** (2006) 123.
- [46] B. E. Schaefer, APJ **583** (2003) L67.
- [47] Z. G. Dai, E. W. Liang and D. Xu, APJ **612** (2004) L101.
- [48] G. Ghirlanda, G. Ghisellini, D. Lazzati and C. Firmani, Astrophys.J. **613** (2004) L13.
- [49] C. Firmani, G. Ghisellini, G. Ghirlanda, V. Avila-Reese, Mon.Not.Roy.Astron.Soc. **360** (2005) L1.
- [50] A.S. Friedman, J. S. Bloom, APJ **627** (2005) 1.
- [51] D.Q. Lamb et al. , astro-ph/0507362.
- [52] E.W. Liang and B. Zhang, APJ **633** (2005) 611.
- [53] E. Mortsell and J. Sollerman, JCAP **0506** (2005) 009.
- [54] D. Xu, Z.G. Dai and E.W. Liang, Astrophys.J. **633** (2005) 603.
- [55] M. Su, H. Li, Z.H. Fan and B. Liu, astro-ph/0611155.
- [56] B. E. Schaefer, astro-ph/0612285.
- [57] M. Chevallier and D. Polarski, Int. J. Mod. Phys. D **10** (2001) 213;  
E. V. Linder, Phys. Rev. Lett. **90** (2003) 091301.
- [58] A. Lewis and S. Bridle, Phys. Rev. D **66** (2002) 103511.
- [59] W. L. Freedman *et al.*, APJ. **553** (2001) 47.
- [60] S. Burles, K. M. Nollett and M. S. Turner, APJ **552** (2001) L1.
- [61] M. Tegmark *et al.* [SDSS Collaboration], APJ **606** (2004) 702.
- [62] S. Cole *et al.* [The 2dFGRS Collaboration], Mon. Not. Roy. Astron. Soc. **362** (2005) 505.
- [63] M. Tegmark *et al.* [SDSS Collaboration], Phys. Rev. D **69** (2004) 103501.
- [64] C. Firmani, V. Avila-Reese, G. Ghisellini, G. Ghirlanda, Rev. Mex. Astron. Astrofis. **43** (2007) 203.
- [65] E. Di Pietro and J. F. Claeskens, Mon. Not. Roy. Astron. Soc. **341** (2003) 1299.
- [66] M. Goliath, et al., astro-ph/0104009.
- [67] A. Gelman and D. Rubin, Statistical Science **7** (1992) 457.